First-Principles Study of Two-Dimensional Titanium Dioxides

Hisako Sato,[†,⊥] Kanta Ono,[*,‡,⊥] Takayoshi Sasaki,[§,⊥] and Akihiko Yamagishi[†,⊥]

Department of Earth and Planetary Science, Graduate School of Science, The University of Tokyo, Hongo, Tokyo 113-0033, Japan, Institute of Materials Structure Science, High Energy Accelerator Research Organization (KEK), Tsukuba, Ibaraki 305-0801, Japan, and Advanced Materials Laboratory, National Institute for Materials Science, Tsukuba, Ibaraki 305-0044, Japan

Received: April 16, 2003; In Final Form: June 13, 2003

Stacked and single-layered lepidocrocite-type titanium dioxides (hereafter denoted as single-layered and stacked TiO_2's, respectively) have been investigated by using first-principles calculations within density functional theory. The crystal structures, electronic structures, dielectric properties, and mechanical properties have been studied. The validity of the present theory was confirmed by reproducing the experimental properties of known bulk TiO_2 polymorphs (rutile and anatase). As for a single-layered lepidocrocite-type TiO_2, the optimized structural parameters agree well with the reported data of an exfoliated nanosheet of $Ti_{0.91}O_2$ or $Cs_{0.7}Ti_{1.825}O_4\square_{0.175}$ ($\square$ = vacancy). Single-layered TiO_2 is slightly less stable than rutile and anatase. The band gap of single-layered TiO_2 is 3.15 eV, which is larger than those of rutile and anatase due to a quantum size effect in a two-dimensional structure with a thickness less than 1 nm. The dielectric constant of the single-layered lepidocrocite-type TiO_2 is highly anisotropic. The elastic constant of single-layered TiO_2 shows an extra flexibility along the sheet normal.

Introduction

Titanium dioxide is one of the most prominent materials in performing various kinds of functions in areas including photocatalysis,[1] photovoltaic cells,[2] electronic devices,[3] and sensors.[4] The semiconducting properties of TiO_2 are essential in accomplishing these functions. Experimental approaches have been reported to control the size or shape of this material toward more advanced applications. One is to scale down its particle size to the nanometer range. This results in an enhancement of the surface area and the photochemical or physical activities with a reduction of light scattering. Another approach is to reduce the dimensionality of the material. A two-dimensional sheetlike shape of TiO_2, for example, provides possibilities for new applications, including an ultrathin film of TiO_2.

With use of the second approach, one of the present authors (T.S.) has succeeded in synthesizing two-dimensional crystallites of titanium dioxide by delaminating a layered titanate.[5−7] These nanosheet-shaped materials can be regarded as a new class of nanoscale semiconductor with a two-dimensional structure.[8,9] The $Ti_{0.91}O_2$ nanosheet shows a very sharp optical absorption peak, which is blue-shifted with respect to bulk TiO_2 due to having originated from a quantum size effect in the nanosheet.[9] These TiO_2 nanosheets, for example, can be artificially deposited layer by layer onto a solid surface to produce a nanostructured assembly.[10] The films are expected to achieve advanced functions, such as uni-directional electron or energy transfer. They may also attain higher efficiency of light-energy conversion by diminishing electron-hole recombination.

Applications of TiO_2 nanosheets as nanoscale functional materials require definite information on its electronic, mechanical, and electric properties. Although a TiO_2 nanosheet is a very attractive material, we are confronted with experimental difficulties in preparing a sample and measuring its physical properties. A theoretical approach is, therefore, strongly motivated for predicting the properties of a TiO_2 nanosheet. Previous theoretical studies on TiO_2 systems have been restricted to the physical properties of popular bulk polymorphs, such as rutile and anatase.[11−17] To the best of our knowledge, there has been no attempt to conduct theoretical studies of TiO_2 nanosheets. It is of significant interest to clarify how two-dimensional TiO_2 is distinct from three-dimensional polymorphs. In the present study, we performed first-principles calculations for a TiO_2 nanosheet using density functional theory (DFT). We aimed to compare various properties, such as the electronic, mechanical, and dielectric properties, of a single-layered TiO_2 nanosheet and its stacked system with those of rutile and anatase. Although an actual nanosheet of $Ti_{0.91}O_2$ has vacancies and counterions, we hope that theoretical studies on a two-dimensional TiO_2 would help to explore a new field of applications for $Ti_{0.91}O_2$ nanosheets.

Method

The calculations presented here were performed by using the plane-wave pseudopotential software CASTEP.[18] Density-functional theory (DFT) using a local-density approximation (LDA)[19] and a gradient-corrected approximation (GGA), Perdew−Burke−Ernzerhof (PBE) functional,[20] were used for the exchange-correlation functional.

For structural optimization, an electronic structure calculation, and an elastic constant calculation, electron−core interactions are described by small-core ultrasoft pseudopotentials which have been used for both oxygen and titanium.[21] Valence states include 2s and 2p states for O (6 valence electrons), and 3s, 3p, 3d, and 4s states for Ti (12 valence electrons). An explicit treatment of semicore Ti 3s and 3p states as valence orbitals

* To whom all correspondence should be addressed. E-mail: kanta.ono@kek.jp.
† The University of Tokyo.
⊥ Also at CREST, Japan Science and Technology Corporation.
‡ High Energy Accelerator Research Organization (KEK).
§ National Institute for Materials Science.

10.1021/jp035017t CCC: $25.00
Published on Web 08/16/2003

TABLE 1: Structural Parameters (Lattice Constants *a* and *c*)and Energy Difference for Rutile and Anatase with the Experimental Data[a]

	rutile		anatase		ΔE (eV/TiO_2) =
	a (nm)	*c* (nm)	*a* (nm)	*c* (nm)	$E_{rutile} - E_{anatase}$
exptl[25]	0.4587	0.2954	0.3782	0.9502	
calcd	0.4683	0.2961	0.3792	0.9663	0.2106
	(+2.1%)	(+0.2%)	(+0.3%)	(+1.7%)	

[a] The difference between the calculated and experimental values is shown as a percentage in parentheses.

was found to be important, as was previously shown in studies on the structure of bulk rutile.[22] The smooth parts of the wave functions were expanded in plane waves with a kinetic energy cutoff of 340 eV. The Brillouin-zone sampling was performed by using a Monkhorst-Pack grid with a (5,5,9) grid of *k* points for rutile, (7,7,9) for anatase, (7,7,8) for stacked TiO_2, and (7,8,2) for single-layered TiO_2.[23] Structural optimizations were converged to a displacement of less than 0.0001 nm and an energy difference of less than 1×10^{-5} eV/atom, using a Broyden−Fletcher−Goldfarb−Shanno (BFGS) minimization algorithm.

To calculate the dielectric functions, norm-conserving pseudopotentials were used for oxygen and titanium.[24] Valence states include 2s and 2p states for O (6 valence electrons) and 3d and 4s states for Ti (4 valence electrons). The plane-wave basis set with an energy cutoff of 1500 eV was used for predicting reliable values. Dielectric functions were calculated within the electric-dipole approximation.

Results and Discussion

I. Structure of Stacked Titanium Dioxides of Lepidocrocite-Type. We first calculated the optimized structure for a stacked system of two-dimensional titanium dioxides. Before performing the calculations, the validity of the theory was examined in the cases of rutile and anatase, which are well-known polymorphs of TiO_2. Two different approximations were used for the exchange-correlation functional: one was the PBE functional and the other the LDA. Table 1 gives the optimized structures of rutile and anatase and their energy difference, using the PBE functional with corresponding experimental data.[25] We concluded that the theoretical and experimental data agreed satisfactorily, showing reasonable validity of this treatment for further investigations. Although nearly the same results were obtained with LDA, the PBE provided better results. Hereafter, we only discuss the results obtained with the PBE functional.

We performed a structural optimization for stacked two-dimensional lepidocrocite-type titanium dioxides. The unit cell is defined by a lattice vector (*a*, *b*, and *c*) where the *ab*-plane is a two-dimensional plane, and layers are stacked along the *c*-axis. Although the lepidocrocite-type stacked structure is originally a C-centered orthorhombic with a space group of *Cmcm*, we set the space group of stacked TiO_2 to *Bmmb* to adopt the *ab*-plane as a two-dimensional plane. Figure 1a shows the structure of stacked lepidocrocite-type TiO_2 with a unit cell. The structural parameters and internal coordinates in the unit cell are summarized in Table 2a,b. Each Ti atom is octahedrally coordinated to six O atoms. There are two inequivalent O atoms that are 2-fold (O(1)) and 4-fold (O(2)) coordinated to Ti atoms. The TiO_6 octahedron is considerably distorted with three different Ti−O bond lengths. The shortest bond is Ti−O(1) with a bond length of 0.182 nm. The second shortest bond is Ti−O(2) with a bond length of 0.196 nm. The third bond is Ti to O(2) in the next unit cell with a bond length of 0.223 nm. O(1) is 2-fold coordinated to Ti atoms and the Mulliken atomic charge

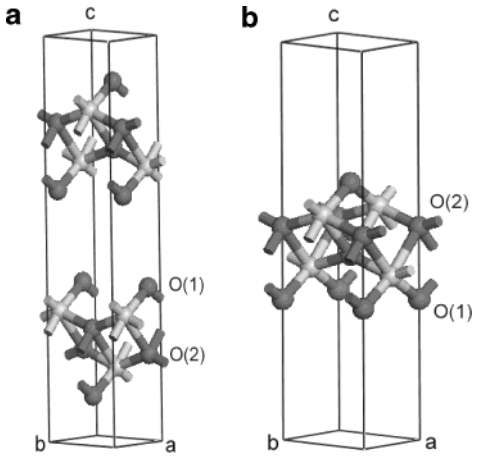

Figure 1. Crystal structures of (a) a stacked TiO_2 and (b) a single-layered TiO_2 with a conventional unit cell.

TABLE 2: (a) Structural Parameters (*a*, *b*, and *c*) and (b) Internal Coordinates (*x*, *y*, and *z*) of Stacked and Single-layered Lepidocrocite-Type TiO_2

(a) Structural Parameters

	stacked			single-layered with 1 nm vacuum slab	
	a (nm)	*b* (nm)	*c* (nm)	*a* (nm)	*b* (nm)
calcd	0.3718	0.3029	1.6022	0.3733	0.3029
ΔE[a] (eV /TiO_2)	0.4527			0.4004	

(b) Internal Coordinated

	stacked			single-layered		
	x	*y*	*z*	*x*	*y*	*z*
Ti	0	0.25	0.68009	0	0.5	0.57657
O(1)	0	0.25	0.38322	0	0	0.64632
O(2)	0	0.25	0.21802	0	0	0.46481

[a] $\Delta E = E - E_{anatase}$

is determined to be −0.61. O(2) is 4-fold coordinated to Ti atoms with an atomic charge of −0.73, and plays an important role in the formation of a two-dimensional architecture. The atomic charge of Ti is determined to be 1.34. Comparing the atomic charges of stacked lepidocrocite-type TiO_2 with rutile (1.34(Ti), −0.67(O)) and anatase (1.38(Ti), −0.69(O)), the major difference lies in the presence of an inequivalent O atom, which causes the Ti−O(1) bond to be less ionic than the Ti−O(2) bond. The two-dimensional arrangement of the octahedra parallel to the *ab*-plane leads to the formation of the nanosheet TiO_2.

Total-energy calculations revealed that stacked TiO_2 was a little less stable than anatase and rutile. The difference between stacked two-dimensional TiO_2 and rutile is similar to that between rutile and anatase, indicating that stacked two-dimensional TiO_2 can exist as a metastable phase of TiO_2 polymorphs.

II. Structure of Single-Layered Titanium Dioxide of Lepidocrocite-Type. The structure of a single layer of lepidocrocite-type titanium dioxides (single-layered TiO_2) was examined. Single-layered TiO_2 was modeled as a supercell in which a vacuum slab and two-dimensional TiO_2 alternate. The vacuum slab was inserted to isolate two-dimensional TiO_2 by diminishing interactions between layers. There was no difference between the results with the thickness of the vacuum slab being 1 or 2 nm, or more. Thus, the interactions could be neglected when nanosheets were apart from each other at a distance of 1 nm. Thus, in the calculations on single-layered TiO_2, all of the

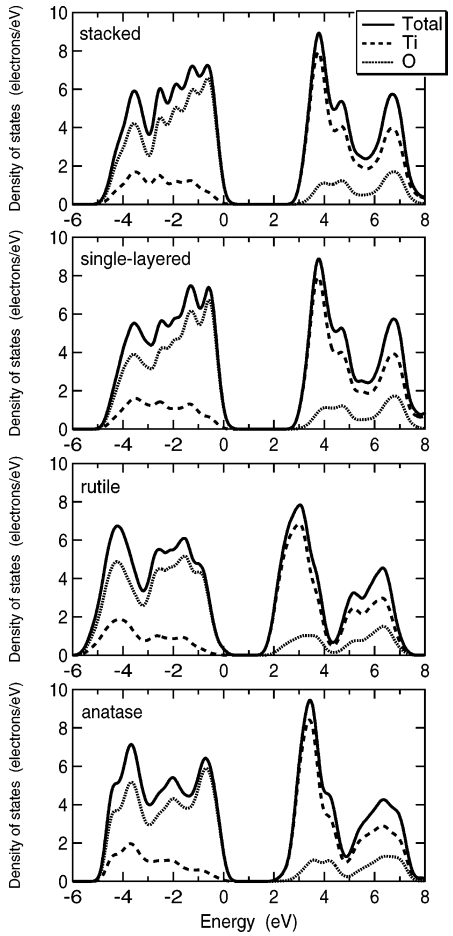

Figure 2. Total and partial density of states for (a) a stacked TiO_2 (b) a single-layered TiO_2, (c) rutile, and (d) anatase.

TABLE 3: Electronic Dielectric Permittivity Tensors of TiO_2

	electronic dielectric constants			exptl	
phase	ϵ_{xx}	ϵ_{yy}	ϵ_{zz}	ϵ_{xx}	ϵ_{zz}
rutile	6.94	6.94	8.22	6.843[a]	8.427[a]
anatase	6.36	6.36	6.05	5.82[b]	5.41[b]
single-layered	6.29	9.60	5.17		

[a] Data from ref 28. [b] Data from ref 29.

results were conducted with a 1 nm thick vacuum slab. The symmetry of a structure is reduced to *Pmmn*. The unit cell contains two TiO_2 units and the *ab*-plane is a two-dimensional plane. Figure 1b depicts the structure of single-layered TiO_2. The optimized structural parameters and internal coordinates are summarized in Table 2a,b. The structure of the single-layered TiO_2 is almost the same as that of the stacked TiO_2, where the positions of the Ti and O atoms are identical within 0.001 nm. The Ti−O bond lengths (0.182, 0.196, and 0.222 nm) and the atomic charges [1.36(Ti), −0.62(O(1)), and −0.74(O(2))] are also in excellent agreement with those of stacked TiO_2. The total energy of single-layered TiO_2 is negligible (0.05 eV/TiO_2), less than that of stacked TiO_2.

The in-plane lattice constant of single-layered TiO_2 (a = 0.3733 nm; b = 0.3029 nm) is formed to be very similar to the experimental cell parameters (0.38 nm × 0.30 nm) of a molecular nanosheet crystallite of $Ti_{0.91}O_2$ derived from $Cs_{0.7}Ti_{1.825}O_4\square_{0.175}$ (□, vacancy) via delamination.[9] This reasonable agreement suggests that the starting point for the prediction of the physical properties of a single-layered TiO_2 nanosheet based on this model should be acceptable.

III. Electronic Structures. The total and partial densities of states of single-layered and stacked TiO_2 are shown in Figure 2. There is a considerable resemblance between the densities of states of single-layered TiO_2 (Figure 2b) and their stacked form (Figure 2a). The main contribution to the valence band is O 2p states that are bonding with Ti 3d. The conduction band is decomposed into Ti 3d e_g states (5−8 eV) and t_{2g}-states (2−5 eV) that are antibonding with O 2p, and the main contribution to the conduction band is Ti 3d t_{2g}-states. The density of states of single-layered TiO_2 and its stacked form are considerably different from that of rutile (Figure 2c). On the other hand, there is a similarity in the density of states among stacked, single-layered TiO_2's and anatase (Figure 2d) except for a difference in the band gap. The resemblance in the conduction band indicates similar crystal-field splitting and bonding characteristics in Ti 3d states for stacked, single-layered TiO_2's and anatase.

The band gap was determined to be 3.15 eV for both stacked and single-layered TiO_2's, which is larger than those of rutile (2.28 eV) and anatase (2.67 eV). In the band structures of stacked and single-layered TiO_2's, no band dispersion is observed along the c^*-axis in the Brillouin zone. In contrast, a large band dispersion is observed parallel to the sheet-plane (*ab*-plane) in the reciprocal space, indicating highly anisotropic two-dimensional electronic structures in stacked and single-layered TiO_2's. The larger band gap is considered to be ascribed to a quantum size effect or to the lower dimensionality. In two-dimensional systems, the bandwidth becomes narrower than that in three-dimensional systems because the transfer integrals are smaller in a two-dimensional sheet than in a three-dimensional bulk material. Although it is well-known that the DFT calculation in LDA or GGA underestimates the band gap, the trend of a larger band gap in two-dimensional TiO_2, both stacked and single-layered, compared with rutile and anatase is essential.[26]

IV. Dielectric Properties. Dielectric properties are important for semiconductor device applications. The imaginary part of the dielectric function was calculated within the electric-dipole approximation, where transitions between occupied and unoccupied electronic states are calculated, and the real part was transformed from the imaginary part by using the Kramers−Kronig transformation. No attempt for correcting the under-

TABLE 4: Experimental and Calculated Elastic Constants of TiO_2

C_{ij} (GPa)	rutile[a] exptl	rutile calcd	anatase calcd	stacked calcd	single-layer calcd
C_{11}	268.0 ± 1.4	261.1 ± 5.3	311.2 ± 5.9	162.5 ± 3.4	97.3 ± 1.5
C_{22}	268.0 ± 1.4	261.1 ± 5.3	311.2 ± 5.9	270.3 ± 0.9	150.0 ± 0.9
C_{33}	484.2 ± 1.8	455.8 ± 2.8	190.8 ± 2.6	−1.4 ± 3.3	−2.1 ± 4.9
C_{44}	123.8 ± 0.2	117.2 ± 2.2	50.8 ± 5.5	5.7 ± 2.1	2.1 ± 2.5
C_{55}	123.8 ± 0.2	117.2 ± 2.2	50.8 ± 5.5	7.8 ± 5.5	1.4 ± 3.7
C_{66}	190.2 ± 0.5	203.7 ± 1.9	59.4 ± 0.99	68.1 ± 0.4	36.2 ± 0.1
C_{12}	174.9 ± 1.4	132.1 ± 4.6	150.3 ± 3.8	57.1 ± 2.5	28.9 ± 0.8
C_{13}	147.4 ± 1.5	136.7 ± 4.6	137.6 ± 2.7	6.7 ± 2.5	0.5 ± 2.3

[a] Data from ref 31.

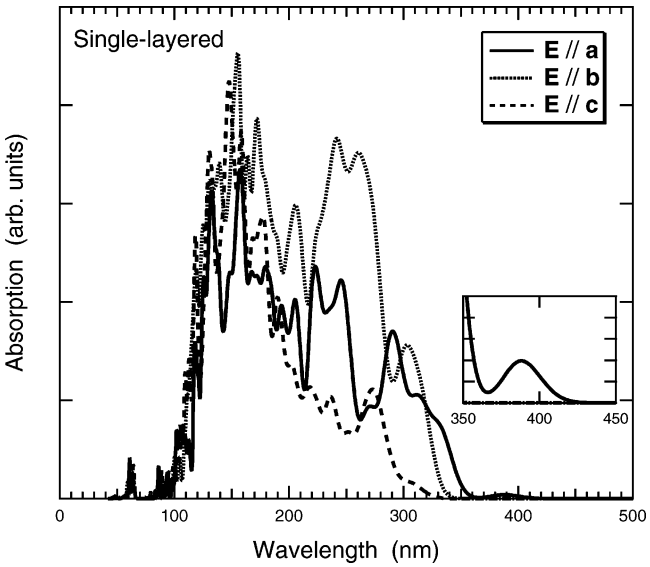

Figure 3. Calculated optical absorption spectra of a single-layered TiO_2 as a function of wavelength and polarization.

estimated band gap was made in this study.[27] For single-layered TiO_2, the effective dielectric constant (ϵ_{eff}) is determined from

$$\epsilon_{eff}(\omega) = (\epsilon(\omega)t_c - \dot{\epsilon}_v t_v)/t \quad (1)$$

where t_c, t_v, and t are the length of the *c*-axis of the unit cell (1.45274 nm), the thicknesess of the vacuum slab (1.0 nm), and the thickness of single-layered TiO_2 (0.45274 nm), respectively; ω is a frequency and $\dot{\epsilon}$ and $\dot{\epsilon}_v$ are the calculated dielectric constants of the unit cell and vacuum ($\epsilon_v = 1$), respectively.

The calculated electronic dielectric constants at $\omega \rightarrow 0$ of rutile, anatase, and single-layered TiO_2 were compared with the experimental data (Table 3). The calculated electronic dielectric constants of rutile show good agreement with the experimental values.[26,27] The calculated electronic dielectric constants of anatase are about 10% larger than the experimental values. The smaller electronic dielectric constant in rutile compared with anatase is consistent with the experimental data.[28,29]

The dielectric constants of single-layered TiO_2 are anisotropic and are related to the crystal structure and mechanical properties. The in-plane dielectric constants of single-layered TiO_2 are similar to those of rutile and anatase, suggesting a promising possibility of applications as dielectric materials. Although the static (low frequency) dielectric constant is more important than the electronic (high frequency) dielectric constant in device applications, it is rather difficult to calculate the static dielectric constant because of the close coupling with the lattice dynamics. Further theoretical calculations are needed for this purpose.

Figure 3 shows the calculated optical absorption spectra of single-layered TiO_2 as a function of the light wavelength and polarization. Highly anisotropic optical absorption was found. A small preabsorption edge at around 400 nm was only found for polarization parallel to the *a*-axis, indicating that the band-gap transitions from the p-state to the t_{2g}-state are dipole-allowed for the $\boldsymbol{E}||\mathbf{a}$ polarization and dipole-forbidden for the $\boldsymbol{E}\perp\mathbf{a}$ polarization. The main absorption edge around 300 nm is allowed for both the $\boldsymbol{E}||\mathbf{a}$ and $\boldsymbol{E}||\mathbf{b}$ polarizations, and comparably agrees with the experimental data for a $Ti_{0.91}O_2$ nanaosheet.[5,8] A large blue shift is observed for the $\boldsymbol{E}||\mathbf{c}$ polarization. This blue shift originates from a quantum size effect in two-dimensional nanosheets where an electronic structure along the *c*-axis is discrete. It is concluded that the overall calculated spectral features reproduce considerably well the experimental data.[8]

V. Mechanical Properties. Although the mechanical properties of the TiO_2 nanosheet are interesting and important, it is difficult to measure those properties, particularly for such nanoscale materials. Recent state-of-the-art calculations enable the calculation of the mechanical properties based on DFT. It is known that the accuracy of the DFT elastic constants is typically within 10% or less compared with the experimental values. In this study, the elastic constants of two-dimensional TiO_2 as well as rutile and anatase were calculated. To examine the accuracy of the present theory, the bulk moduli of rutile and anatase were calculated by using the PBE functional and compared with the experimental bulk moduli.[30,31] The calculated bulk modulus of anatase (171.4 ± 1.7 GPa) agrees very well with that of the experimental data (179 ± 2 GPa)[31] with an error of less than 5%. On the other hand, the bulk modulus of rutile (187.2 ± 2.6 GPa) is rather smaller than the experimental data (211.5 ± 2.2 GPa) by about 13%. It should be noted that the accuracy of these calculations is much better than other recent first-principles calculations.[12]

Since the bulk modulus is not a good index for mechanical properties in two-dimensional systems, we consider the elastic constant tensor of stacked and single-layered lepidocrocite-type TiO_2's. The elastic constant tensors (C_{11}, C_{22}, C_{33}, C_{44}, C_{55}, C_{66}, C_{12}, and C_{13}) of rutile, anatase, and stacked and single-layered TiO_2 are listed in Table 4. The calculated elastic constants of rutile agree very well with the experimental data.[31] In the stacked and single-layered TiO_2's, there is an exceedingly high flexibility along the sheet normal, reflecting the two-dimensional nature in TiO_2 nanosheets. The in-plane elastic constant along the *b*-axis is larger than that along the *a*-axis because of the tighter Ti−O bonds, and is related to the larger dielectric constants in ϵ_{yy}. The overall elastic constants of stacked TiO_2 are about 1.8-times larger than these of single-layered TiO_2, indicating an enhancement of the mechanical strength by stacking the two-dimensional sheets.

Conclusion

We investigated the structural, electronic, mechanical, and optical properties of two-dimensional titanium dioxides using first-principles calculations within density functional theory. The present theoretical study would be helpful in exploring a novel class of nanosheet titanium oxides as functional materials.

Acknowledgment. This work has been supported by CREST of JST (Japan Science and Technology Corporation). This work has been financially supported by a Grant-in-Aid for scientific Research on Priority Areas (417) from the Ministry of Education, Culture, Sports, Science and Technology (MEXT) of the Japanese Government.

References and Notes

(1) Fujishima, A.; Honda, K. *Nature (London)* **1972**, *238*, 37.
(2) Bach, U.; Lupo, D.; Comte, P.; Moser, J. E.; Weiss, F.; Salbeck, J.; Spreitzer, H.; Gratzel, M. *Nature* **1998**, *395*, 583.
(3) Wagemaker, M.; Kentgens, A. P. M.; Mulder, F. M. *Nature* **2002**, *418*, 397.
(4) Wu, N.-L.; Wang, S.-Y.; Rusakova, L. A. *Science* **1999**, *285*, 1375.
(5) Sasaki, T. Novel Nanosheet Crystallites and Their Layer by-Layer Assembly. In *Handbook of Polyelectrolytes and Their Application*; Tripathy, S., Kumor, J., Nalwa, H. S., Eds.; American Scientific Publishers: Stevenson Ranch, CA, 2002; Vol. 1, pp 241−263.
(6) Sasaki, T.; Watanabe, M.; Hashizume, H.; Yamada, H.; Nakazawa, H. *J. Am. Chem. Soc.* **1996**, *118*, 8329.
(7) Sasaki, T.; Watanabe, M. *J. Am. Chem. Soc.* **1998**, *120*, 4682.
(8) Sasaki. T.; Watanabe M. *J. Phys. Chem. B* **1997**, *101*, 10159.

(9) Sasaki, T.; Ebina, Y.; Kitami, Y.; Watanabe, M.; Oikawa, T. *J. Phys. Chem. B* **2001**, *105*, 6116.
(10) Sasaki, T.; Ebina, Y.; Tanaka, T.; Harada, M.; Watanabe, M. *Chem. Mater*. **2001**, *13*, 4661.
(11) Lazzeri, M.; Vittaddini, A.; Selloni, A. *Phys. Rev. B* **2001**, *63*, 155409.
(12) Muscat, J.; Swamy, V.; Harrison, M. *Phys. Rev. B* **2002**, *65*, 224112.
(13) Swamy, V.; Gale, J. D. *Phys. Rev. B* **2000**, *62*, 5406.
(14) Lazzer, M.; Selloni, A. *Phys. Rev. Lett.* **2001**, *87*, 266105.
(15) Asahi, R.; Taga, Y.; Mannstadt, W.; Freeman, A. J. *Phys. Rev. B* **2000**, *61*, 7459.
(16) Mikami, M.; Nakamura, S.; Kitap, O.; Arakawa, H. *Phys. Rev. B* **2002**, *66*, 155213.
(17) Koudrachova, M. V.; Harrison, N. M.; de Leeuw, S. W. *Phys. Rev. B* **2002**, *65*, 235423.
(18) Segall, M. D.; Lindan, P. L. D.; Probert, M. J.; Pickard, C. J.; Hasnip, P. J.; Clark, M. C.; Payne, M. C. *J. Phys.* **2002**, *14*, 2717.
(19) Ceperley, D. M.; Alder, B. J. *Phys. Rev. Lett.* **1980**, *45*, 566.
(20) Perdew, J. P.; Burke, K.; Ernzerhof, M. *Phys. Rev. Lett.* **1996**, *77*, 3865.
(21) Vanderbilt, D. *Phys. Rev.* **1990**, *B41*, 7892.
(22) Paxton, A. T.; Thien-Nga, L. *Phys. Rev.* **1998**, *B57*, 1579.
(23) Monkhorst, H.; Pack, J. D. *Phys. Rev.* **1976**, *B13*, 5188.
(24) Lin, J. S.; Qteish, A.; Payne, M. C.; Heine, V. *Phy. Rev.* **1993**, *B47*, 4174.
(25) Burdtt, J. K.; Hughbanks, T.; Miller, G. J.; Richardson, J. W., Jr.; Smith, J. K. *J. Am. Chem. Soc.* **1987**, *109*, 3639.
(26) Perdew. J. P.; Zunger, A. *Phys. Rev. B* **1981**, *30*, 3460.
(27) Gonze. X.; Lee, C. *Phys. Rev. B* **1997**, *55*, 10355.
(28) Traylor, J. G.; Smith, H. G.; Nicklow, R. M.; Wilkinson, M. K. *Phys. Rev. B.* **1971**, *3*, 3457.
(29) Gonzalez, R. J.; Zallen, R.; Berger, H. *Phys. Rev. B* **1997**, *55*, 7014.
(30) Arlt, T.; Bermejo, M.; Blanco, M. A.; Gerward, L.; Jiang, J. Z.; Olsen, J. S.; Recio, J. M. *Phys. Rev. B* **2000**, *61*, 14414.
(31) Isaak, D. G.; Carnes, J. D.; Anderson, O. L.; Cynn, H.; Hake, E. *Phys. Chem. Miner*. **1998**, *26*, 31.